THE ULTRASTRUCTURE OF Z DISKS FROM WHITE, INTERMEDIATE, AND RED FIBERS OF MAMMALIAN STRIATED MUSCLES

R. W. D. ROWE

From the CSIRO Division of Food Research, Meat Research Laboratory, Cannon Hill, Queensland, Australia

ABSTRACT

The Z disk ultrastructure of white, intermediate, and red fibers from mammalian muscle is examined. Three models are proposed that explain the differences between the three types of Z disk. The three models are all based on the same concept, i.e., looping filaments from both sides of the Z disk. The differences between the models are in terms of the spatial relationships of adjacent loops within the Z disk. In the white fiber Z disk model all the loops from one side of the Z disk are on the same plane. In intermediate fibers there are two planes of loops from both sides of the Z disk, whereas in red fibers there are three planes of loops from both sides. The implications of these three structures are discussed in relation to known physiological differences between the fiber types.

INTRODUCTION

The classification of striated muscle fiber types has been attempted using a number of parameters including histochemical, biochemical, morphological, and physiological differences. Although this work has been carried out over a number of years and the amount of data collected is voluminous, there is still no clear classification that satisfies all the parameters. Some workers have used classifications with as many as eight different fiber types (Romanul and Hogan, 1964), whereas the minimum number appears to be three (Gauthier, 1969). The structural criteria used to separate fiber types were originally derived from light microscope observations (Ranvier, 1873, 1874). More recently, electron microscopy has enabled a number of ultrastructural differences to be defined which appear to be specific for the three (white, intermediate, and red) fiber types (Padykula and Gauthier, 1967 *b*).

In most of the published work relating to morphological differences between fiber types, the differences between the Z disks are stressed. White fibers have the thinnest Z disks and red fibers, the thickest, with intermediate fiber Z disks between these extremes (Schiaffino et al., 1970; Padykula and Gauthier, 1967 *a*; Gauthier, 1969). Although these differences between Z disks have been known for some time and are very striking, an explanation of the basic structural differences between them is lacking from the literature. A considerable amount of work has been devoted to working out theories of Z disk ultrastructure, but all of this work has aimed at an explanation of images of thin Z disks comparable to those of white fibers (Knappeis and Carlsen, 1962; Franzini-Armstrong and Porter, 1964; Reedy, 1964; Kelly, 1967; Landon, 1970; Macdonald and Engel, 1971; Rowe, 1971; Kelly and Cahill, 1972).

The whole problem of Z disk structure is complicated by the lack of an absolute answer to the structure of the thin (and therefore simpler

structure?) Z disks as seen in white fibers. Much of the debate as to which of the present interpretations of Z disk images is the closest to the in vivo structure stems from the different images produced by different fixation techniques. The work presented here is an attempt to throw some light on the structural differences between Z disks. It is hoped the work will show that, although there are differences between types of Z disks, there are also enough similarities to make it necessary to bear in mind all three Z disk types when considering an explanation of the ultrastructure of any one of them. The functional significance of different Z disk ultrastructure is also considered in the light of known differences between fiber types.

MATERIALS AND METHODS

Rat plantaris muscle was exposed and fastened to a wooden toothpick while still attached to the leg at both the origin and insertion and with the ankle joint fully dorsiflexed. The muscle was then cut free from the leg and fixed for 2 h at 0°C in mixed glutaraldehyde (2.5%) and osmium tetroxide (1%) fixative buffered to pH 7.3 with 0.1 M cacodylate buffer (Hirsch and Fedorko, 1968). After fixation, short lengths of the surface fibers of the muscle were removed and washed overnight in several changes of 0.1 M cacodylate buffer (pH 7.3), and the rest of the muscle was discarded. After dehydration in a graded ethanol series at 4°C the tissue was infiltrated with epoxy propane followed by embedding in Araldite. Thin sections cut with glass knives were stained in uranyl acetate (saturated solution in 50% ethanol) and Reynolds' (1963) lead citrate. Sections were examined in a Philips EM300 electron microscope. In some instances linear integration of the micrographs of Z disks was carried out. The technique used was essentially that of Markham et al. (1964; see also Horne, 1965). The image of the Z disk was moved by one I filament-I filament spacing between successive exposures.

RESULTS

The general morphological features characteristic of a particular fiber type have been dealt with by previous workers (Padykula and Gauthier, 1967 *a*; Gauthier, 1969) and will not be listed here. This paper is concerned only with the differences between the Z disks, which in themselves are characteristic and distinctive for the three fiber types (see Introduction). The classification of the fibers examined here was on the basis of these morphological differences.

Figs. 1–3 show white, intermediate, and red fibers, respectively. The variation in the appearance of the internal structure within Z disks from neighboring myofibrils of the same fiber is the result of viewing a square lattice with two planes of symmetry at 45° to one another at angles ranging from 0 to 45° relative to these planes. This is the case for the Z disks of white, intermediate, and red fibers. Only with views corresponding to the two planes of symmetry can any semblance of order be seen. The view along one of these planes shows the I filaments on either side of the Z disk to be out of phase by 50% and is the view indicated in Fig. 1 (single arrow; see also Figs. 2 and 3). A view along the other plane of symmetry shows the I filaments to be apparently continuous through the Z disk (double arrows, Figs. 1 and 3). From Figs. 1–3, the differences between the Z disks of the three fiber types are immediately obvious. White fiber Z disks (Fig. 1) are the thinnest of the three types (Schiaffino et al., 1970). They also show the most consistent thickness and run in straight lines at right angles to the long axis of the myofibril. The apparent thickness of the white fiber Z disk is not affected by section thickness in excess of 22 nm when viewed in true longitudinal section. The only source of variance in Z disk thickness is the angle of the plane of section. Intermediate fiber Z disks (Fig. 2) are clearly of greater but less constant thickness than white fiber Z disks. In this case, as is the case for red fiber Z disks, the apparent thickness of the Z disks can be influenced by the section thickness to a certain extent and by the longitudinal level at which the Z disk is sectioned. This is because of the nature of the Z disk structure and the effect will become apparent later when the structure has been described. The red fiber Z disks (Fig. 3) are the thickest of the three types. They also show the greatest apparent variation in thickness and the course taken by them is often far from a straight line at right angles to the long axis of the myofibril (Fig. 3, asterisks).

At higher magnifications structural details of the Z disks are revealed. In order to enhance the structural appearance of the Z disks, a linear integration technique similar to that of Markham et al. (1964) has been used on three of the Z lines shown here (Figs. 5, 7, and 9). One interpretation of white fiber Z disk structure which has been reported in detail elsewhere (Rowe, 1971) used a looping filament concept to explain the structure. This is the model used in the present paper.

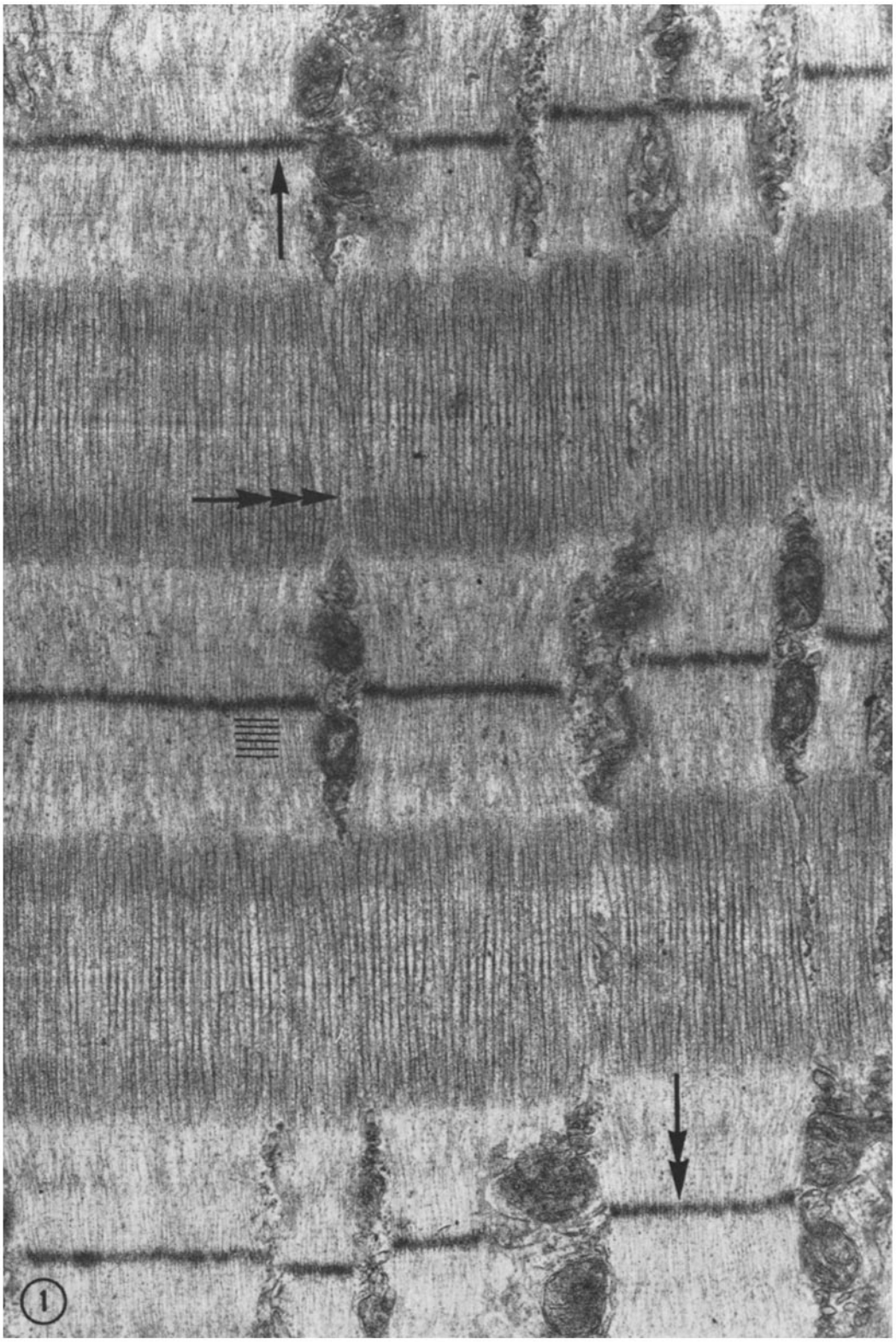

FIGURE 1 A longitudinal section of a white fiber showing the thin straight Z disks at right angles to the long axis of the fiber. Single and double arrows show the two views of the Z disk in longitudinal section along the two planes of symmetry of the square lattice. The triple arrow shows the relatively sharp demarcation line of the ends of the I filaments within the A band. Horizontal bars show the 40 nm periodicity of the I band. × 32,000.

FIGURE 2 A longitudinal section of an intermediate fiber showing the intermediate thickness Z disks. For an explanation of the single arrow and horizontal bars, see Fig. 1. × 32,000.

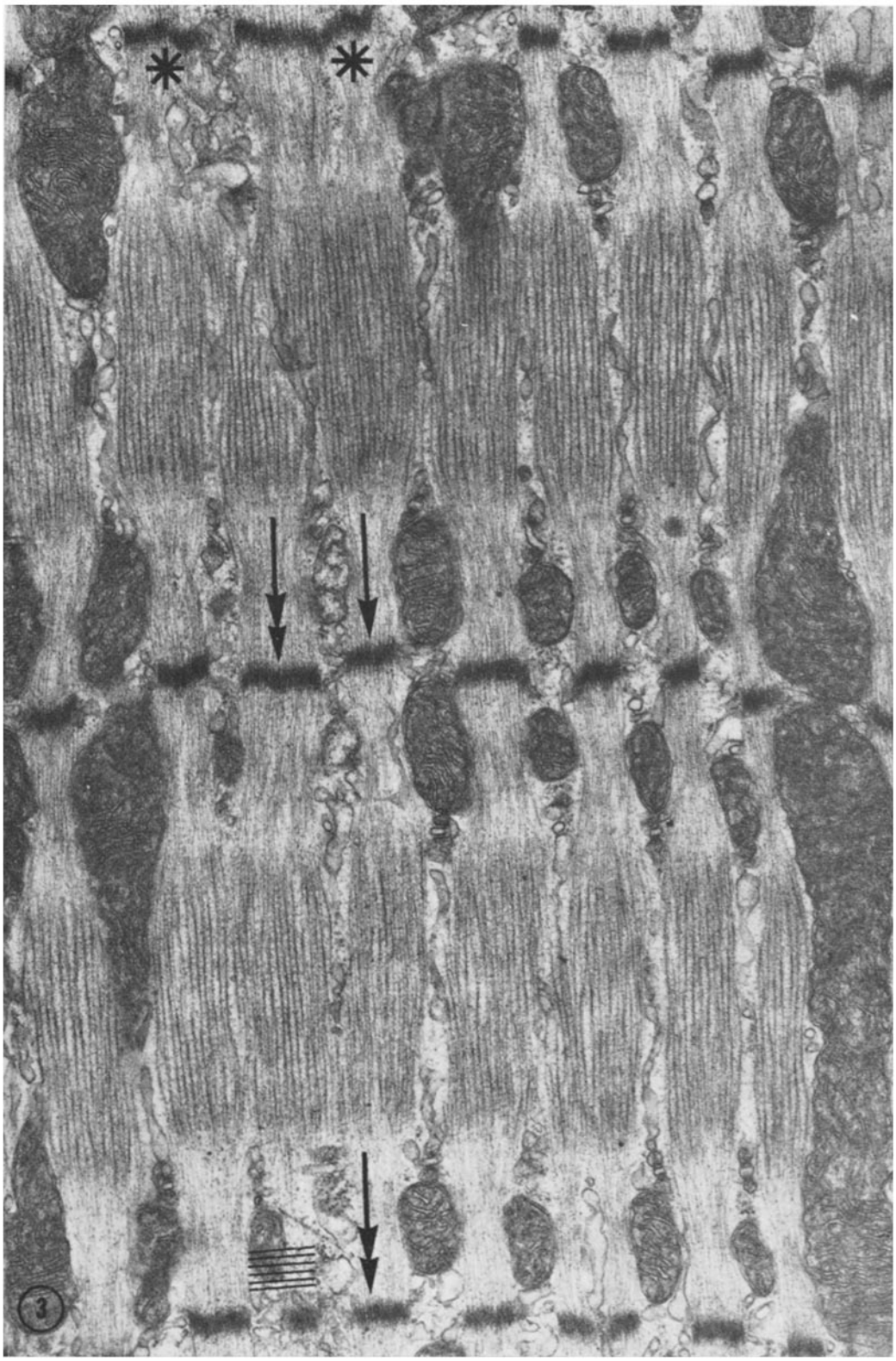

FIGURE 3 A longitudinal section of a red fiber. Note the thick Z disks often showing an erratic course (asterisks) relative to the long axis of the fiber. For an explanation of the single and double arrows and the horizontal bars, see Fig. 1. The triple arrow shows the indiscrete line of I filament cutoff within the A band (cf. Fig. 1). × 32,000.

However, other models of Z disk ultrastructure (white fiber type) can be adapted. These include the looping filament model of Kelly (1967), the nonlooping filament models of Knappeis and Carlsen (1962), Reedy (1964), Macdonald and Engel (1971), and the model of Kelly and Cahill (1972) which draws attention to the Z matrix component of the Z disk as applied to both looping and nonlooping filament models. Only the structural details of the model used here (Rowe, 1971) and those that are relevant to the present paper will be dealt with.

The I filaments, or extensions from them, from one side of the Z disk overlap with the I filaments from the other side, within the Z disk thickness. The ends of adjacent filaments from the same side of the Z disk are linked by loops (Figs. 10 A, 4, and 5). This gives the impression of a double row of chevrons (bars, Figs. 4 and 5) running transverse to the I filaments (these are best seen by viewing the micrographs at an acute angle). The spacing between the two rows of chevrons is constant. Fig. 10 A is a model showing the positions of the I filaments and Z loops of a white fiber, with x as the spacing of the chevrons. Because tissue-handling techniques can cause an appreciable amount of shrinkage and compression (Page, 1964; Page and Huxley, 1963), the actual measurements of distance x are not really meaningful. However, it can be said that in the tissue examined the value of x was the same as the spacing of the transverse periodicity seen in I bands and identified as the sites of troponin-tropomyosin complexes on the I filaments (Ohtsuki et al., 1967). Therefore, if the amount of shrinkage is the same in the I band and the Z disk then an in vivo value for x would be approximately 40 nm.

Sections of intermediate fiber Z disks at high magnification reveal a somewhat more complicated structure (Figs. 6 and 7). The I filaments again overlap within the Z disk thickness but in this case the ends of the adjacent I filaments, from the same sarcomere, appear in some places to be linked by loops on two planes[1] (bars, Figs. 6 and 7). In this situation the appearance is very similar to two white fiber Z disks side by side. The spacings of the triple row of chevrons are constant and adjacent chevrons are separated by the same distance as those of white fiber Z disks (i.e., x). Fig. 10 B shows a model with the positioning of the loops and I filaments in an intermediate fiber Z disk. In some instances (Fig. 6, brackets) the appearance of the Z disk changes from this triple chevron typical of intermediate fibers to an apparent double-chevron arrangement identical with that found in white fibers.

Comparable micrographs of red fiber Z disks are shown in Figs. 8 and 9. The appearance is of three white fiber Z disks in series giving a total of four rows of chevrons (Figs. 8 and 9, bars). This has been interpreted as three planes of looping attachments between I filaments from the same side of the Z disk. The three planes from each side superimpose such that two planes from each side are common to both whereas the third and leading plane for each is mutually exclusive. The model shown in Fig. 10 C shows this spacing of the chevrons; the spacing is again constant and equal to x of Fig. 10 A and B.

In some places (Fig. 8, brackets) the four-chevron appearance of the red fiber Z disk gives way to a three-chevron picture reminiscent of the intermediate fiber Z disk. When extremely thin sections of red fiber Z disks are examined, then the four rows of chevrons seen in Fig. 8 give way to an appearance not unlike situations seen in white fiber Z disks. Fig. 11 shows a Z disk from the same fiber as in Fig. 8, but the section in Fig. 11 is so thin as to include only one layer of I filaments from both sides of the Z disk and there is only one plane of loops (arrows) from each side resulting in a much thinner Z disk.

DISCUSSION

Proposed Models of Z Disk Structure

WHITE FIBER Z DISKS: The model proposed for the structure of white fiber Z disks is the simplest of the three. A detailed description of the model has been published elsewhere (Rowe, 1971). In this previous paper (Rowe, 1971) the author used rat soleus muscle. This is a muscle considered to be composed predominantly of red fibers with some intermediate fibers. In an attempt to produce a model of Z disk structure compatible with those previously published, i.e. relatively thin simple structures, the author dismissed as artifact and/or misleading the triple-chevron appearance. Upon reexamination of the material reported in that paper it is obvious that the

[1] "Plane" always refers to a transverse level of the myofibril, whereas "layer" refers to a longitudinal level.

fibers examined were of the intermediate type; indeed, the three rows of chevrons can be seen in Figs. 5 and 6 of Rowe (1971). This fact, however, does not detract from Rowe's (1971) interpretation of Z disk structure because as clearly demonstrated here (Figs. 4 and 6) the appearance of white and intermediate fiber Z disks is in some places identical under certain conditions of section thickness and plane of section. The evidence for the Z disk structure derived from transverse sections would not be affected by being derived from intermediate fiber Z disks. At the Z disk, each I filament joins with four loops (see Fig. 12 A). Each of these loops joins with an adjacent I filament from the same sarcomere forming a 22 nm square mesh (Fig. 12 A). The two meshes, one from each side of the Z disk, are interlocked by virtue of the fact that the two sets of I filaments are offset (see Fig. 1 of Rowe and Morton, 1971) and interdigitate before forming the meshes. Because the meshes from either side of the Z disk are identical structures, further description will be confined mainly to only one mesh (this is also the case for intermediate and red fiber Z disks).

In two dimensions the smallest unit cell of one mesh is one hairpin configuration comprised of two adjacent I filaments linked by a Z loop (e.g. Fig. 10 A and a_1, a_2, b_1, b_2 of Fig. 12 A). The simplicity of the model arises because all the unit cells have the same spatial relationships with their neighbors; i.e., there is only one plane of loops. In three dimensions the smallest unit cell comprises four hairpin configurations arranged in a square lattice (e.g. a_1b_1, a_1b_2, a_2b_1, a_2b_2 of Fig. 12 A).

Fig. 13 A shows three layers of hairpin configurations from each side of the Z disk viewed in longitudinal section. For simplicity, the loops linking the successive layers have been omitted. The shading code of Fig. 13 A corresponds to that of Fig. 12. In Figs. 12 and 13 A all the loops from one side of the Z disk are on the same plane. Therefore in this model no matter how many layers of loops are included in the section thickness, if they are viewed in true longitudinal section they do not alter the apparent thickness of the Z disk and show a maximum of two rows of chevrons (cf. Figs. 10 A, 13 A, 4, and 5).

INTERMEDIATE FIBER Z DISK: A diagram of the mesh from one side of the intermediate fiber Z disk model is shown in Fig. 12 B. In two dimensions the unit cell is the same as in the white fiber Z disk, i.e., one hairpin configuration. However, adjacent unit cells have the Z loop on different planes, 40 nm apart; i.e. in Fig. 12 B loops of $a_{\text{odd no.}}$ and $b_{\text{even no.}}$ are on the same plane but 40 nm from the plane of $a_{\text{even no.}}$ and $b_{\text{odd no.}}$ loops. In three dimensions the unit cell is again four hairpin configurations in a square cell. Each of these cells has loops on two different planes. The spacing of the loops on the different planes is such that opposite hairpins in the unit cell are on different planes. When the two interlocking meshes, comprising the Z disk, are viewed in longitudinal section, they give rise to three rows of chevrons (Figs. 10 B, 6, and 7).

Above a section thickness with sufficient depth of tissue to include two layers of loops from each side of the Z disk, the apparent thickness of the Z disk does not increase. If the section thickness is reduced so that only two layers from one side and one from the other are included, then only two rows of chevrons will remain, i.e., apparent white fiber Z disk thickness. This can be achieved by visualizing Fig. 13 B without the three deepest layers of loops, i.e., both solid dark loops and the dotted loop from the left (cf. bracketed regions

---

FIGURES 4–9 High magnification longitudinal views of Z disks from white, intermediate, and red fibers. Figs. 4 (× 251,000) and 5 *a* (× 226,000): white fiber Z disks. The two meshes interlock to give the double-chevron appearance (two bars). The spacing between the planes of loops of the two meshes is constant and corresponds to *x* of Fig. 10 A (cf. Fig. 13 A). Fig. 5 *b*: linearly integrated photograph of the Z disk shown in Fig. 5 *a*. Figs. 6 (× 172,000) and 7 *a* (× 231,000): intermediate fiber Z disks. The spacing between the three rows of chevrons (bars) is the same as in Figs. 4 and 5 *a*, i.e. *x* (cf. Figs. 10 B and 13 B). The bracketed regions show double rows of chevrons comparable to Figs. 4 and 5 *a*; for a full explanation see the text. Fig. 7 *b*: linearly integrated photograph of the Z disk shown in Fig. 7 *a*. Figs. 8 (× 257,000) and 9 *a* (× 164,000): red fiber Z disks. Three planes of loops from each mesh superimpose to give the four rows of chevrons (bars) typical of a red fiber Z disk. The bracketed regions, however, show only three rows of chevrons, i.e. more typical of an intermediate fiber (cf. Figs. 6 and 7); for a full explanation see the text. Fig. 9 *b*: linearly integrated photograph of the red fiber Z disk shown in Fig. 9 *a*.

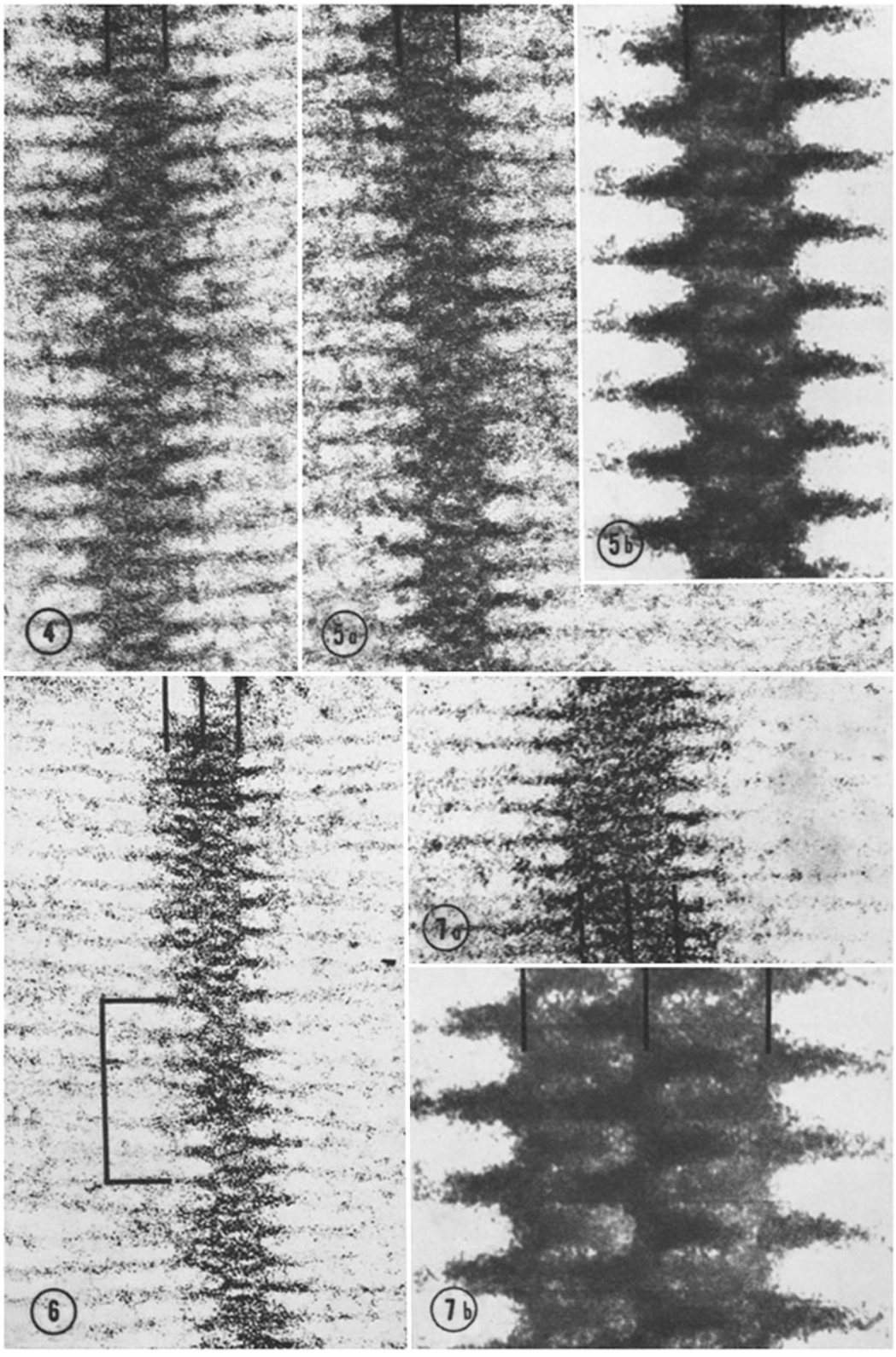
4
5a
5b
6
7a
7b

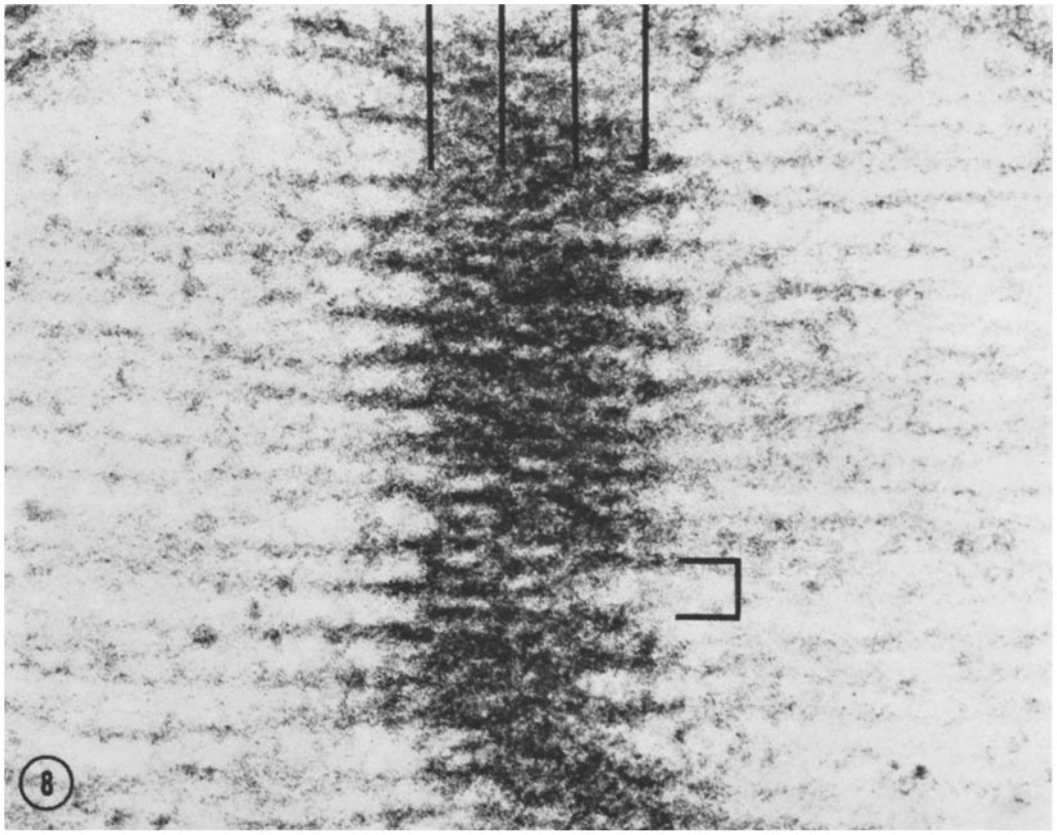
8

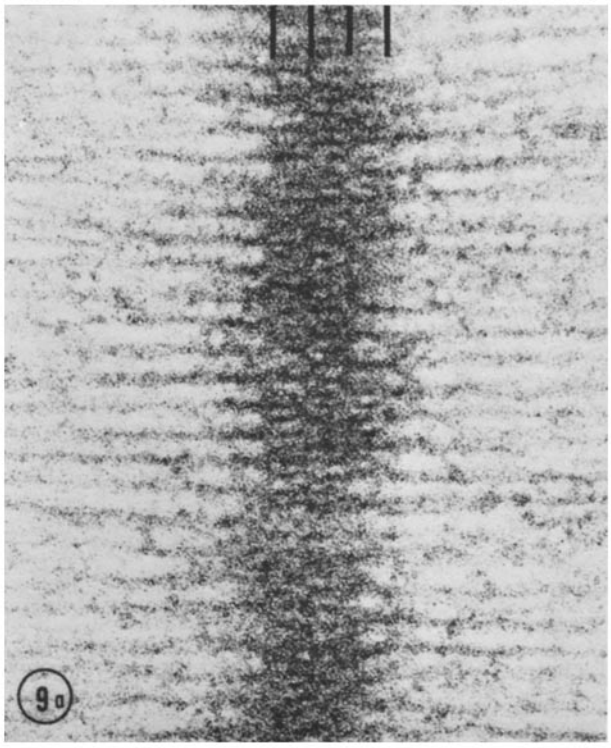
9a

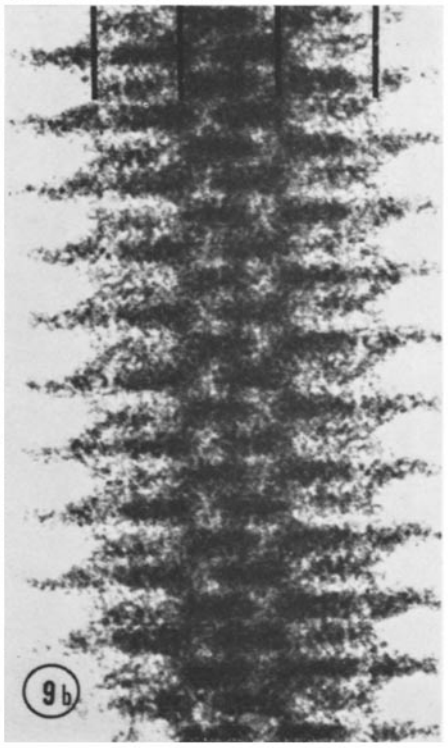
9b

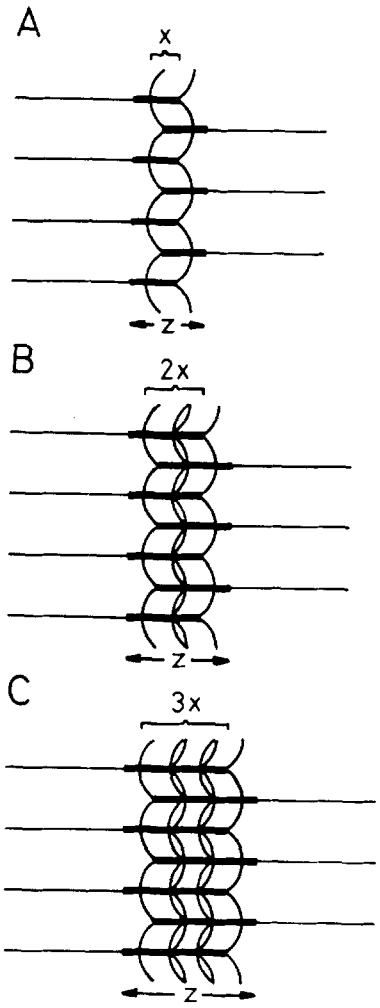

FIGURE 10 A, B, and C show the appearance of white, intermediate, and red fiber Z disk models, respectively, seen in longitudinal section. In A, all of the loops from one side of the Z disk lie on the same plane and are a constant distance (x) from the loops from the other side, giving a double row of chevrons (cf. Figs. 4 and 5). In B, individual loops can exist on one of two planes. Each loop is, however, still a constant distance (x) from the matching loop from the other side. Therefore, when successive layers of loops superimpose, there appear to be three rows of chevrons (cf. Figs. 6 and 7). The red fiber model C takes this concept one step further. Here there are three planes of loops from each side with a constant distance (x) between loops from opposite sides, giving four rows of chevrons (cf. Figs. 8 and 9).

of Fig. 6). Alternatively the same effect, i.e. alternation between inclusion of two layers from both sides with two from one side and one from the other, can be achieved within a section of uniform thickness by moving the plane of section slightly off parallel to the square lattice of the Z disk (see Fig. 14). Here, although the section thickness is maintained uniform and of sufficient depth to accommodate two layers of I filaments from both sides of the Z disk (left-hand side of Fig. 14) because the plane of section is not quite parallel with the Z lattice, there are only two layers of I filaments from one side and one from the other side of the Z disk included in the section on the right of Fig. 14. Therefore, slight variation in the section thickness and/or angle of the plane of section, relative to the lines of symmetry of the square lattice of the Z disk, can give rise to the variation in intermediate fiber Z disk structure seen in the microscope including apparent discrepancies in Z disk thickness.

RED FIBER Z DISK: Red fiber Z disks appear the most complicated of the three types examined. The basic unit of one mesh is still a hairpin configuration in two dimensions (e.g. a_1, a_2, b_1, b_2, b_3 of Fig. 12 C). In this model there are three planes of loops, and adjacent loops in the same axis are separated by one plane interval, x of Fig. 10 (i.e., 40 nm). In three dimensions the unit cell is again four hairpin configurations in a square lattice (Fig. 12 C). Each unit cell has loops on only two planes, with opposite loops of the cell on different planes one plane interval apart. This means that for the three planes to be incorporated, adjacent cells (in three dimensions) have one plane common to both cells (the middle plane and the other planes of the two cells are 80 nm ($2x$) apart (the leading plane and the trailing plane, respectively); e.g. cell a_1b_1 (Fig. 12 C) has loops on the leading plane and middle plane, whereas its neighboring cells a_2b_1 and a_1b_2 have loops on the middle plane and trailing plane.

Fig. 13 C shows a longitudinal view of three layers of loops from this mesh and from the mesh from the other side of the Z disk. For a view of the red fiber Z disk at its greatest thickness the section has to be thick enough to accommodate three layers of loops from both sides of the Z disk (in some levels of section four layers of loops are needed; see below). Sections thicker than this do not increase the apparent thickness of the Z disk or the maximum of four rows of chevrons. Thinner sections can reduce the apparent thickness of the Z disk. The effects of the section thickness on the apparent thickness of the Z disk can be seen by visualizing Fig. 13 C and mentally masking out the deeper layers of loops. Removal of the two

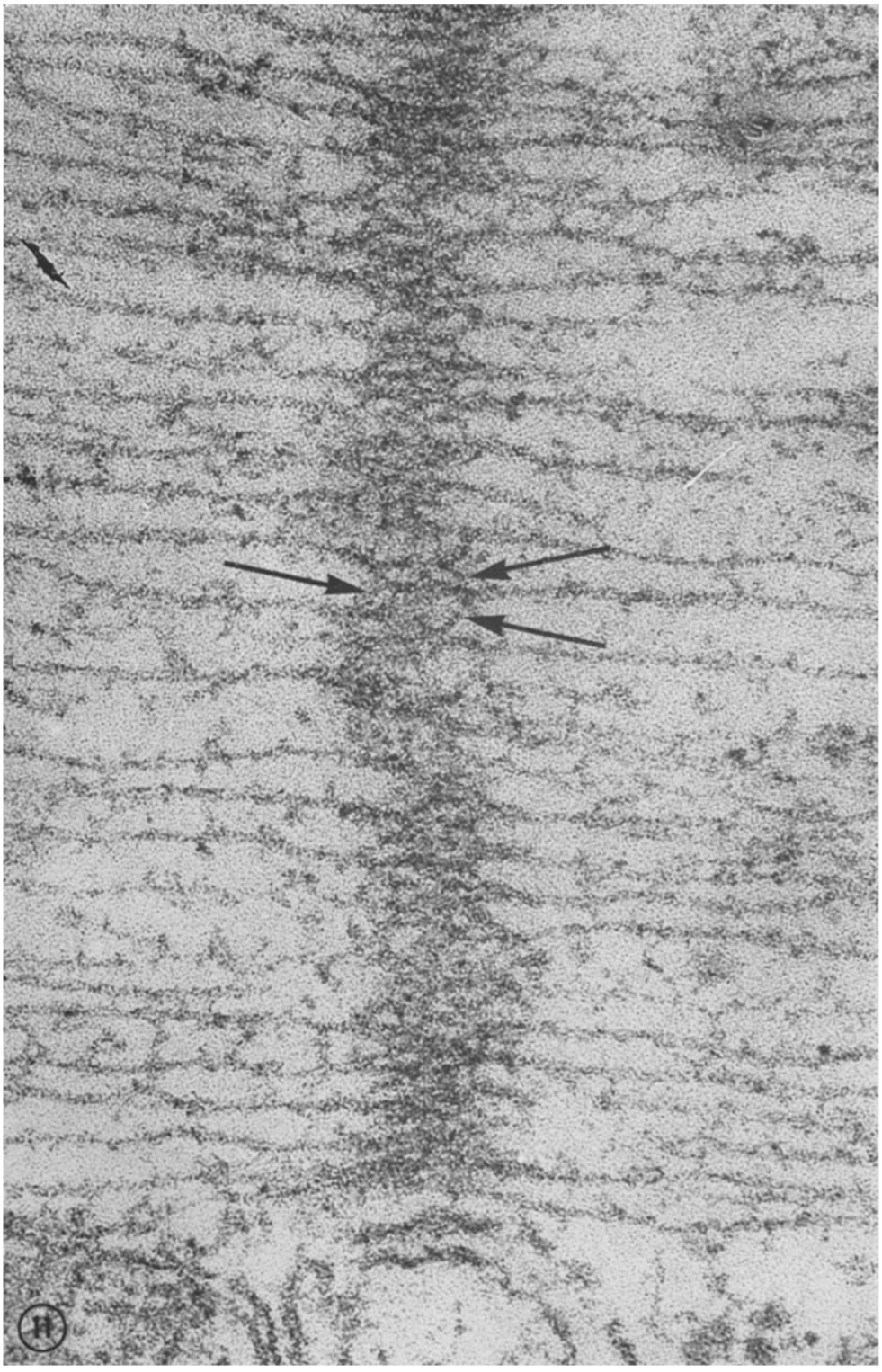

FIGURE 11 This micrograph shows a longitudinal section of a red fiber Z disk from the same fiber as the Z disk shown in Fig. 8. The difference between the two appearances results from differences in the section thickness. In Fig. 8 there are two or three layers of loops from each side of the Z disk superimposed, whereas in Fig. 13 the section is sufficiently thin to include only slightly in excess of one layer of loops from each mesh. Arrows show individual Z loops. × 237,000.

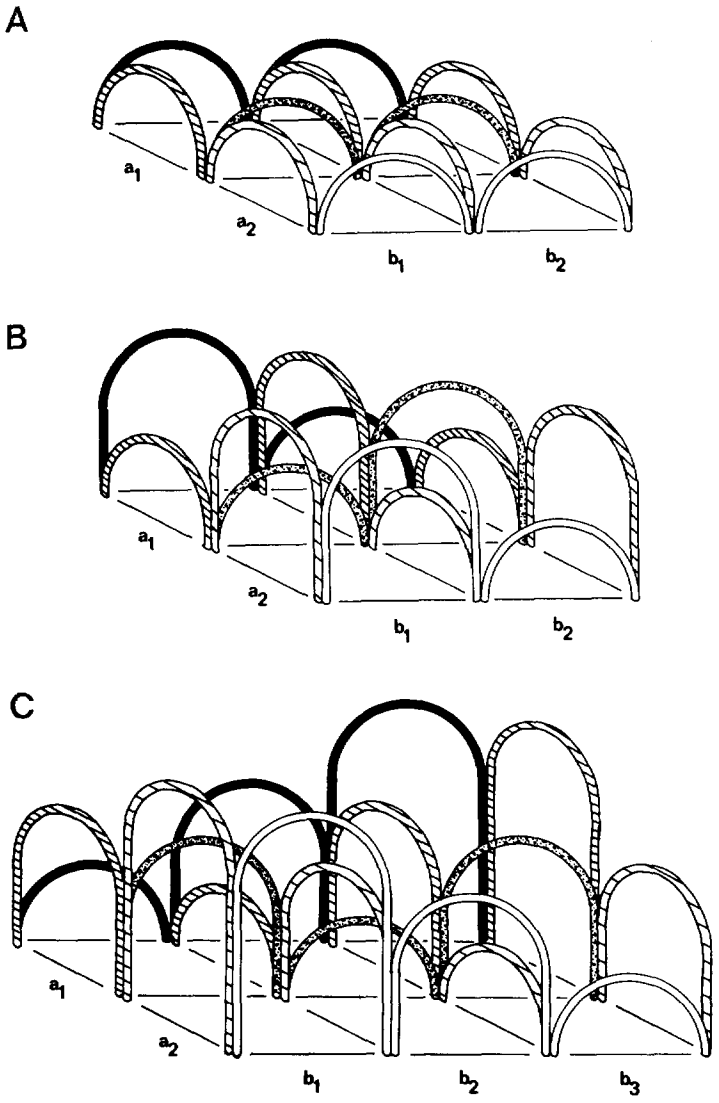

FIGURE 12 A, B, and C show diagrammatically the three-dimensional appearance of one mesh of the Z disk for white, intermediate, and red fibers, respectively. $a_{1\ldots n}$ and $b_{1\ldots n}$ show the basic two-dimensional hairpin structures. $a_{1\ldots n}$ $b_{1\ldots n}$ give the unit cell structures in three dimensions. (A) White fiber Z disks have all the loops of the mesh on the same plane. (B) Z loops of intermediate fiber Z disks exist on one of two planes, 40 nm apart; adjacent loops along one axis (a or b) of the lattice are always on different planes. (C) Z loops of red fiber Z disks exist on one of three planes, 40 nm apart; adjacent loops along one axis of the lattice are always on different planes and move successively from the leading plane (b_1) through the middle plane (b_2) to the trailing plane (b_3); b_4, if it were shown, would be at the middle plane, etc.

deepest layers (solid black loops) produces an intermediate fiber Z disk appearance (cf. Fig. 13 B and bracketed regions of Figs. 8 and 9). Removal of the four deepest layers (solid black and dotted loops) produces a white fiber Z disk appearance (cf. Figs. 13 A and 11). As with intermediate fiber Z disks slight variation in the angle of the plane of section can also affect the apparent Z disk thickness. The level at which the section is taken relative to the three planes of loops also has

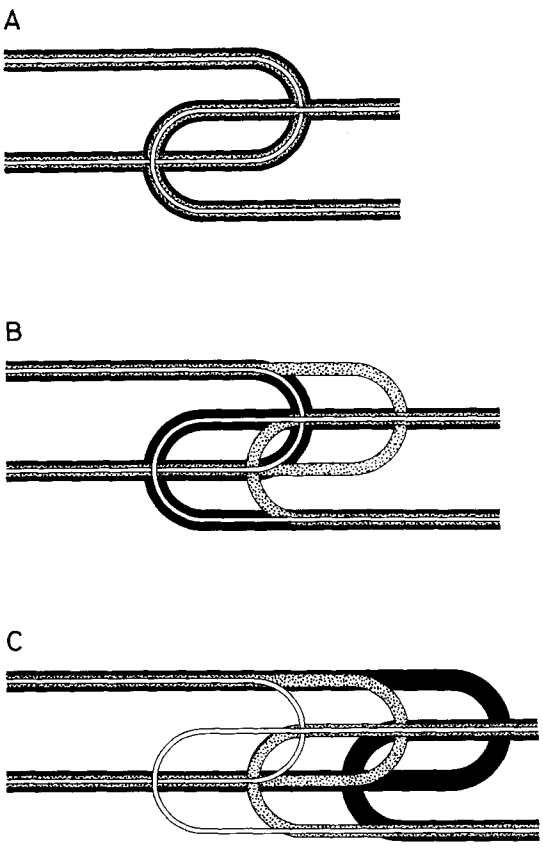

FIGURE 13 This diagram is a more detailed explanation of Fig. 10. A, B, and C show three layers of loops for the two meshes (shading code is equivalent to shading of loops in Fig. 12) superimposed in longitudinal section. (A) In white fiber Z disks all loops from one side of the Z disk superimpose, resulting in the double-chevron appearance of the Z disk (cf. Figs. 10 A, 12 A, 4, and 5). (B) Successive layers of loops of the meshes from intermediate fiber Z disks are on different planes, resulting in the three rows of chevrons (cf. Figs. 10 B, 12 B, 6, and 7). (C) The three planes of loops for each mesh (from each side of the Z disk) superimpose to give the four rows of chevrons seen in red fiber Z disks (cf. Figs. 10 C, 12 C, 8, and 9).

important implications on the appearance of the red fiber Z disk in longitudinal sections. If a section thick enough to contain three layers of loops from both sides is considered then from Fig. 12 C when the three layers are as those of the b_1 row, three planes of loops are represented. However, if the three layers are as those of the b_2 row, then only two of the three planes of loops are shown. In this latter case, four layers would be required to show the three planes of loops.

The linear integration technique used here to enhance the Z disk images should be capable, given a suitable image to work with, of demonstrating the differences between the effects of section thickness on the appearance of the three Z disk types. Starting with sections of the three types thin enough to include only one layer of loops from each side of the Z disk, i.e. with apparent Z disk thickness the same for all three types, linear integration should reconstitute the three different structures proposed here. However, for the technique to work there has to be fairly good order in the appearance of the working image over a number of successive loops. To date the author has not been successful in attempts to integrate images from thin sections. Thicker sections are in fact already enhanced images as a result of reinforcement of the Z disk image by superimposition of the layers of loops contained within the section thickness. Therefore linear integration of a thick section image enhances the structural appearance by a factor of y (where y is the number of layers of loops in the section thickness) for each successive exposure. In thin sections where $y = 1$, the number of exposures which have to be made is far greater, thereby requiring greater areas of ordered Z disk in the working print.

The original paper by the author on this type of model (Rowe, 1971) took into account the helical pitch of the components of the I filaments. For the sake of clarity this has not been included in the present paper. However, the helical configuration of these filaments and the loops in the Z disk are easily incorporated but would make the description of them far too long and complicated. Other models of thin (white fiber type) Z disk ultrastructure, including the looping filament model of Kelly (1967) and the nonlooping Z filament models of Knappeis and Carlsen (1962), Reedy (1964), Macdonald and Engel (1971), and the looping-nonlooping-matrix model of Kelly and Cahill (1972) can be adapted, some more easily than others, to explain the three types of Z disk structure reported here. Arguments as to which of these models is the nearest to the in vivo structure will not be discussed here.

It has been shown that, although the three types of Z disk structure differ from one another in a consistent fashion, there are enough similarities between them to warrant explanations of their structure employing a common concept. Indeed, the search for the answer as to the true in vivo

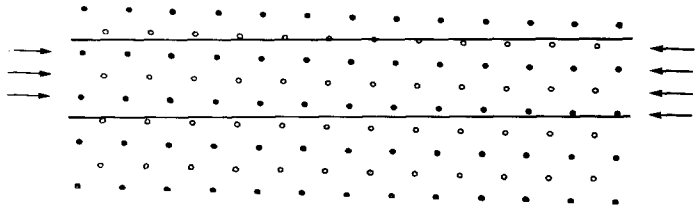

FIGURE 14 Diagram showing the effect of a slight mismatch between the plane of section and the square lattice of the Z disk on the number of layers of I filaments included in a section of uniform thickness (see text).

structure of any one of the three would almost certainly be more easily forthcoming by studying all three types simultaneously. One aspect of the structure of Z disks as reported here remains problematical. In the linearly integrated photographs there is apparently a break in the I filaments where they cross the Z loops. This break is not always present in the nonintegrated photograph (cf. Figs. 5 *a* and *b*, 7 *a* and *b*, 9 *a* and *b*). This could be an artifact resulting from phase eflects present in the working image which have been enhanced by the integration and photographic processing. The integration technique also has the effect of increasing contrast. This can clearly be seen in Fig. 9 *b* in which the central unit of the three repeating units in series is much darker. The middle plane of Z loops from one side and the trailing plane from the other side superimpose to define the central unit, whereas the outer margins of the other units are defined only by the leading plane of Z loops, i.e., half as many loops superimposed resulting in less contrast. The Z matrix, which has long been known to be associated with the filamentous component of the Z disk, is partially responsible for the high contrast of the Z disk. This matrix may be differentially deposited within the Z disk (see Kelly and Cahill, 1972) and in this way contributes to the contrast differences seen in Z disks and highlighted by the integration technique. Under the conditions of exposure and photographic processing employed in the production of Figs. 5 *b*, 7 *b*, and 9 *b*, the I filaments which are reasonably clear in the corresponding working images (Figs. 5 *a*, 7 *a*, and 9 *a*) did not show up.

In studies of this nature where the author is attempting to describe in vivo structures in terms which can be applied to a model or models of the system(s) being examined, there is always the tendency to ignore, if not overlook, slight deviations from the main pattern. However, it should always be remembered that there are often exceptions to the rule, especially in in vivo systems. Presumably the more complex the system the more open to "mistakes" it becomes. Therefore it could be expected that the red fiber Z disk described here would be the one most open to mistakes. One possible mistake is in the sequence of the planes of Z loops. The model described here shows the loops as being in a well ordered sequence, i.e. trailing plane, middle plane, leading plane, middle plane, trailing plane, middle plane, etc. Occasionally, however, a shift occurs in the whole of the Z disk such that the leading plane of loops at one point becomes the middle plane in a neighboring region (see Fig. 15). Similar shifts can and do occur in Z disks of intermediate and white fibers but at a diminishing frequency.

Three clearly distinguishable Z disk structures have been observed in muscle fibers within rat plantaris muscle; each of these clear-cut structures together with other structural features of the fiber in which it occurs makes it appear very likely that each is characteristic of one of the three types of muscle fiber already recognized in muscle, i.e. white, intermediate, and red. The nature of the models proposed here for the three different Z disk structures imposes other characteristics on the three fiber types. Native actin filaments from mammalian striated muscle are considered to be of a relatively constant fixed length. If this is so, then because in red fibers (and to a lesser extent in intermediate fibers) the actin filaments insert into the Z disk at three levels (two levels in intermediate fibers), they must end at different levels within the A band of the muscle. Support for this concept comes from Figs. 1 and 3.

Fig. 1 (triple arrow) shows the relatively clear demarcation, within the A band, of the ends of the I filaments of white fiber sarcomeres. There is no comparable sharp distinction for the sarcomeres

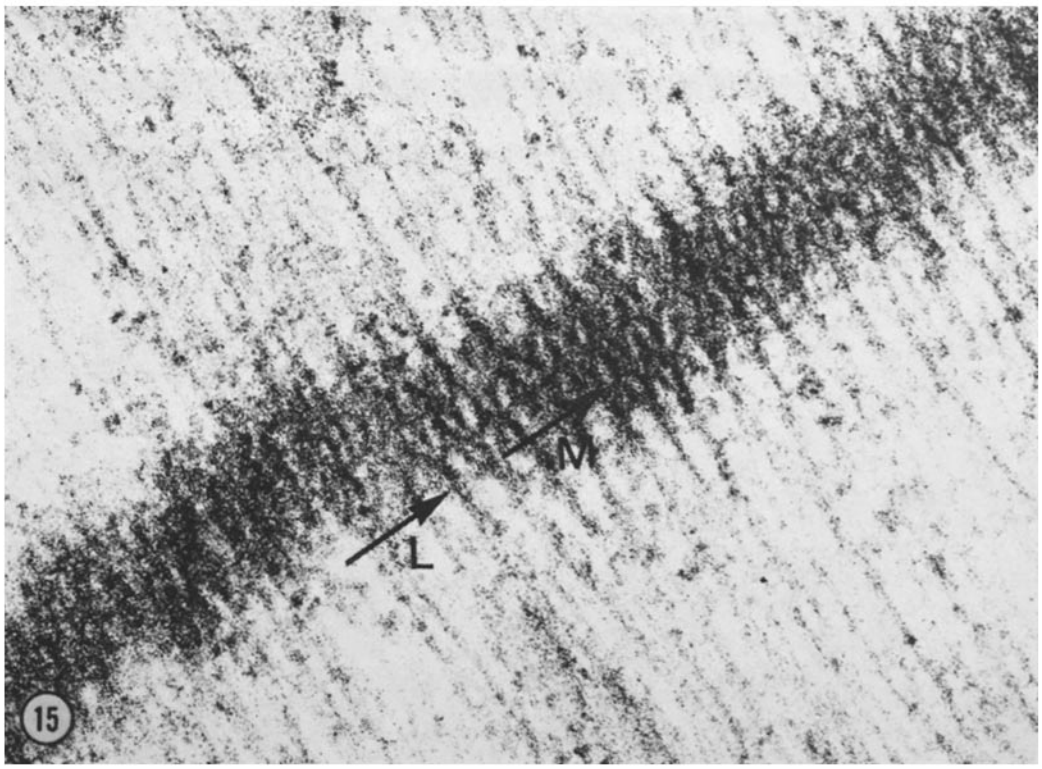

FIGURE 15 Z disk from a red fiber showing a shift in the Z disk such that the leading plane of loops at one point (*L*) becomes the middle plane of loops (*M*) in an adjacent part of the Z disk. × 185,000.

of red fibers (Fig. 3), suggesting that the I filaments do not all terminate in the same plane. The fact that the red fiber Z disks show a tendency not to run in straight lines at right angles to the long axis of the myofibril would also tend to contribute to the smearing of the region of I filament cut off in the A band. The different planes of insertion of I filaments in the Z disk are 40 nm apart. This means that the spatial relationships between the troponin-tropomyosin complexes on the I filaments, which are also spaced at 40 nm intervals along the filament (Ohtsuki et al., 1967), maintain lateral register and can still be seen (bars of Figs. 1, 2, and 3). A sarcomere having I filaments finishing in the A band at different levels (three levels contributed by way of the Z disk structure and a variable amount contributed by the more erratic course of the Z disk relative to the sarcomere long axis [asterisks of Fig. 3]) would be capable of developing tension over a wider range of lengths than would a sarcomere with all the I filaments finishing at the same level.

The work reported by Buller and Lewis (1962) on cat muscle shows that the soleus, a postural muscle (normally looked upon as being composed predominantly of red and intermediate fibers), develops tension over a much wider range of lengths than does the flexor hallucis longus, a phasic muscle (normally having a predominant percentage of white fibers). Rack and Westbury (1969) have shown that the cat soleus muscle develops peak tension at a sarcomere length of 2.8 μm with only a slight drop down to sarcomere lengths of 2.3 μm. Ohtsuki et al. (1967) have shown that there are 24 periodicities in the I band on either side of the Z disk with a repeat distance of 40 nm, i.e. 25 gaps of 40 nm each giving an I filament length of 1 μm. The mechanism being discussed here would have the effect of increasing the effective number of periodicities by two (these would not be visible to count within the I band because the two nearest the Z loops would be masked by the Z disk). This represents an increase in effective I band length of 8%. Such

an increase does not account for all the discrepancy between phasic and postural muscles, but it could contribute to some extent. The tilt of the Z disk discussed below could also increase the effective working range of the sarcomere.

The flexibility of the Z disk would depend to a certain extent on the nature of the interaction of the two interlocked meshes within a single Z disk and on the interaction between these meshes and the associated amorphous matrix. The nature of the meshes proposed here for the three Z disk types has the potential of conferring greater flexibility on the red fiber Z disk than on the white fiber Z disk. This results from the fact that theoretically if the Z loops of the three meshes are straightened out, i.e. the meshes are expanded laterally to their limit, then the meshes of red and intermediate fibers can be expanded to an area slightly less than twice that to which the meshes of white fibers can be expanded. If this is true in vivo, then it would help towards an understanding of some of the differences noted between fiber types, e.g., the tendency for the red fiber Z disk to move away from a straight course at right angles to the long axis of the myofibril. Greater in vivo flexibility of the red fiber Z disks allowing the sarcomere to take on a shape more like that of an obliquely striated muscle (Rosenbluth, 1967), i.e. Z disk inclined at an angle relative to the long axis of the myofibril, would also enable the red fibers to work over a greater range of fiber lengths. Each sarcomere in parallel would contribute an increase in working length proportional to the angle of inclination of the Z disk relative to the long axis of the myofibrils. Increased flexibility of red fiber Z disk would also enable the Z disk to withstand more lateral stress, thereby enabling the red fibers to have myofibrils of greater cross-sectional area than the white fibers (see Goldspink, 1970; Rowe and Morton, 1971). In conclusion, therefore, it can be said that the functional significance of the three types of Z disks described here could have far-reaching effects on the properties of the three fiber types.

I wish to thank Miss Vailele Ledward and Mrs. Sue Tucek for their skillful technical assistance.

This work was supported in part by the Australian Meat Research Committee.

Received for publication 5 September 1972, and in revised form 27 November 1972.

REFERENCES

BULLER, A. J., and D. M. LEWIS. 1962. Factors affecting the differentiation of mammalian fast and slow muscle fibers. *In* The Effect of Use and Disuse on Neuromuscular Functions. E. Gutmann and P. Hnik, editors. Czechoslovak Academy of Science, Prague. 149.

FRANZINI-ARMSTRONG, C., and K. E. PORTER. 1964. The Z disc of skeletal muscle fibrils. *Z. Zellforsch. Mikrosk. Anat.* **61**:661.

GAUTHIER, G. F. 1969. On the relationship of ultrastructural and cytochemical features to colour in mammalian skeletal muscle. *Z. Zellforsch. Mikrosk. Anat.* **95**:462.

GOLDSPINK, G. 1970. The proliferation of myofibrils during muscle fiber growth. *J. Cell Sci.* **6**:593.

HIRSCH, J. G., and M. E. FEDORKO. 1968. Ultrastructure of human leukocytes after simultaneous fixation with glutaraldehyde and osmium tetroxide and "postfixation" in uranyl acetate. *J. Cell Biol.* **38**:615.

HORNE, R. W. 1965. Negative staining methods. *In* Techniques for Electron Microscopy. D. H. Kay, editor. Blackwell Scientific Publications Ltd., Oxford. 352.

KELLY, D. E. 1967. Models of muscle Z-band fine structure based on a looping filament configuration. *J. Cell Biol.* **34**:827.

KELLY, D. E., and M. A. CAHILL. 1972. Filamentous and matrix components of skeletal muscle Z-disks. *Anat. Rec.* **192**:623.

KNAPPEIS, G. G., and F. CARLSEN. 1962. The ultrastructure of the Z disc in skeletal muscle. *J. Cell Biol.* **13**:323.

LANDON, D. N. 1970. The influence of fixation upon the fine structure of the Z-disk of rat striated muscle. *J. Cell Sci.* **6**:257.

MACDONALD, R. D., and A. G. ENGEL. 1971. Observations on organization of Z-disk components and on rod-bodies of Z-disk origin. *J. Cell Biol.* **48**:431.

MARKHAM, R., J. H. HITCHBORN, G. J. HILLS, and S. FREY. 1964. The anatomy of the tobacco mosaic virus. *Virology.* **22**:342.

OHTSUKI, I., T. MASAKI, T. NONOMURA, and S. EBASHI. 1967. Periodic distribution of troponin along the thin filaments. *J. Biochem. (Tokyo).* **61**:817.

PADYKULA, H. A., and G. F. GAUTHIER. 1967 *a.* Ultrastructural features of three fiber types in the rat diaphragm. *Anat. Rec.* **157**:296.

PADYKULA, H. A., and G. F. GAUTHIER. 1967 *b.* Morphological and cytochemical characteristics of fiber types in normal mammalian skeletal muscle. *In* Exploratory Concepts in Neuromus-

cular Dystrophy and Related Disorders. *Excerpta Med. Int. Congr. Ser.* No. 147. 117.

PAGE, S. G. 1964. Filament lengths in resting and excited muscles. *Proc. R. Soc. Lond. B Biol. Sci.* **160**:460.

PAGE, S. G., and H. E. HUXLEY. 1963. Filament lengths in striated muscle. *J. Cell Biol.* **19**:369.

RACK, P. M. H., and D. R. WESTBURY. 1969. The effects of length and stimulus rate on tension in the isometric cat soleus muscle. *J. Physiol. (Lond.).* **204**:443.

RANVIER, L. 1873. Proprietes et structures differentes des muscles rouges et des muscles blancs chez les lapins et chez les raies. *C. R. Hebd. Seances Acad. Sci. Ser. D. Sci. Nat. (Paris).* **77**:1030.

RANVIER, L. 1874. De quelques faits relatifs a l'histologie et a la physiologie des muscles stries. *Arch. Physiol. Norm. Pathol.* **6**(No. 2 Ser. 1):1.

REEDY, M. K. 1964. The structure of actin filaments and the origin of the axial periodicity in the I-substance of vertebrate striated muscle. *Proc. R. Soc. Lond. B Biol. Sci.* **160**:458.

REYNOLDS, E. S. 1963. The use of lead citrate at high pH as an electron-opaque stain in electron microscopy. *J. Cell Biol.* **17**:208.

ROMANUL, F. C. A., and E. L. HOGAN. 1964. Enzymes in muscle. I. Histochemical studies of enzymes in individual muscle fibers. *Arch. Neurol.* **2**:355.

ROSENBLUTH, J. 1967. Obliquely striated muscle. III. Contraction mechanism of *Ascaris* body muscle. *J. Cell Biol.* **34**:15.

ROWE, R. W. D. 1971. Ultrastructure of the Z-line of skeletal muscle fibers. *J. Cell Biol.* **51**:674.

ROWE, R. W. D., and D. J. MORTON. 1971. Faults in the square lattice of mammalian skeletal muscle Z-disks. *J. Cell Sci.* **9**:139.

SCHIAFFINO, S., V. HANZLIKOVA, and S. PIEROBON. 1970. Relations between structure and function in rat skeletal muscle fibers. *J. Cell Biol.* **47**:107